Modeling effect of initial soil moisture on sorptivity and infiltration

Citation	Stewart, R. D., D. E. Rupp, M. R. Abou Najm, and J. S. Selker (2013), Modeling effect of initial soil moisture on sorptivity and infiltration, Water Resources Research, 49, 7037–7047. doi:10.1002/wrcr.20508
DOI	10.1002/wrcr.20508
Publisher	American Geophysical Union
Version	Version of Record
Citable Link	http://hdl.handle.net/1957/47891
Terms of Use	http://cdss.library.oregonstate.edu/sa-termsofuse

WATER RESOURCES RESEARCH, VOL. 49, 7037–7047, doi:10.1002/wrcr.20508, 2013

Modeling effect of initial soil moisture on sorptivity and infiltration

Ryan D. Stewart,[1] David E. Rupp,[2] Majdi R. Abou Najm,[3] and John S. Selker[1]

Received 14 February 2013; revised 23 August 2013; accepted 27 August 2013; published 28 October 2013.

[1] A soil's capillarity, associated with the parameter sorptivity, is a dominant control on infiltration, particularly at the onset of rainfall or irrigation. Many mathematical models used to estimate sorptivity are only valid for dry soils. This paper examines how sorptivity and its capillary component (as wetting front potential) change with initial degree of saturation. We capture these effects with a simple modification to the classic Green-Ampt model of sorptivity. The modified model has practical applications, including (1) accurately describing the relative sorptivity of a soil at various water contents and (2) allowing for quantification of a soil's saturated hydraulic conductivity from sorptivity measurements, given estimates of the soil's characteristic curve and initial water content. The latter application is particularly useful in soils of low permeability, where the time required to estimate hydraulic conductivity through steady-state methods can be impractical.

Citation: Stewart, R. D., D. E. Rupp, M. R. Abou Najm, and J. S. Selker (2013), Modeling effect of initial soil moisture on sorptivity and infiltration, *Water Resour. Res.*, *49*, 7037–7047, doi:10.1002/wrcr.20508.

1. Introduction

[2] Because infiltration affects water availability for vegetation, groundwater recharge, overland flow, and solute transport, it has been the focus of considerable study over the previous century [e.g., *Green and Ampt*, 1911; *Philip*, 1957b; *Wooding*, 1968; *Brutsaert*, 1977]. Under normal conditions, gravity and capillarity drive vertical infiltration, whereas capillarity alone drives horizontal infiltration [*Philip*, 1957b].

[3] Under constant head conditions, one- and three-dimensional vertical infiltration into a uniform soil has been adequately described using *Philip*'s [1957b] two-term approximation:

$$I = S\sqrt{t} + Ct \tag{1}$$

where I is cumulative infiltration over time t and S is the soil sorptivity. For one-dimensional vertical infiltration, C is proportional to the soil's saturated hydraulic conductivity (K_s). The ratio C/K_s is ≤ 1, depending on soil type and soil moisture [*Philip*, 1990], with proposed ranges of $1/3 \leq C/K_s \leq 2/3$ [*Fuentes et al.*, 1992] or $0.3 \leq C/K_s \leq 0.4$ [*Philip*, 1990]. In the case of three-dimensional infiltration, C incorporates both saturated hydraulic conductivity and sorptivity [*Smettem et al.*, 1995; *Touma et al.*, 2007].

[4] At early times (i.e., $t << S^2/C^2$) sorptivity dominates the infiltration behavior, and for very early times ($t \to 0$) the second term on the right hand side may be neglected [*White et al.*, 1992]. Conversely, the second term dominates as time increases, subject to the limit of $t = S^2/C^2$, when the series expansion from which equation (1) was derived is no longer accurate. Alternate expressions have been developed to describe long-time (steady-state) infiltration behavior [*Philip*, 1957a, 1957b; *Wooding*, 1968; *Haverkamp et al.*, 1994], which lend themselves to estimations of K_s. However, the time required to reach late-time or quasi-steady state conditions may be impractical, particularly for soils with low hydraulic conductivity, and assumptions of homogeneity are typically violated for long infiltration experiments.

[5] Infiltration typically occurs over intermediate or transient timescales (neither exclusively early- nor late-time) and is three-dimensional. One such example is infiltration from an axisymmetric single ring source, which can provide a rapid and low-cost measurement of soil hydraulic properties [*Braud et al.*, 2005]. However, interpretation of these infiltration tests often requires that the S and C terms both be considered. Methods to differentiate between sorptivity and saturated hydraulic conductivity for such infiltration conditions have been proposed [*Smiles and Knight*, 1976; *Smettem et al.*, 1995; *Vandervaere et al.*, 2000], but may be inadequate for estimating small K_s values [*Smettem et al.*, 1995].

[6] Sorptivity represents the soil's ability to draw water [*Philip*, 1957b; *Touma et al.*, 2007], which is a function of the capillarity (the driving force) and the soil's hydraulic conductivity (the dissipation). This dual-dependence is evident in *Parlange* [1975]'s precise solution for sorptivity (as modified for positive ponded conditions by *Haverkamp et al.* [1990]):

$$S^2 = 2K_s(\theta_s - \theta_r)(1 - \Theta_0)h_{surf} + (\theta_s - \theta_r)\int_{h_0}^{0}(1 + \Theta - 2\Theta_0)K(h)dh \tag{2}$$

[1]Biological & Ecological Engineering Department, Oregon State University, Corvallis, Oregon, USA.
[2]Oregon Climate Change Research Institute, College of Earth, Ocean and Atmospheric Sciences, Oregon State University, Corvallis, Oregon, USA.
[3]Civil & Environmental Engineering Department, American University of Beirut, Beirut, Lebanon.

Corresponding author: R. D. Stewart, Department of Crop and Soil Environmental Science, Virginia Polytechnic Institute and State University, Blacksburg, VA, USA. (ryan.stewart@vt.edu)

0043-1397/13/10.1002/wrcr.20508

where Θ is the degree of saturation

$$\Theta = \frac{\theta - \theta_r}{\theta_s - \theta_r}, \tag{3}$$

[7] θ_0, θ_s, and θ_r are the initial, saturated, and residual volumetric soil water contents, respectively, $K(h)$ is the hydraulic conductivity as a function of soil matric potential, h_0 is the initial matric potential, and h_{surf} is the depth of ponding at the surface.

[8] Hydraulic conductivity also appears in the simpler or "traditional" definition of sorptivity provided by the *Green and Ampt* [1911] model:

$$S^2 = \frac{2K_s(\theta_s - \theta_r)(1 - \Theta_0)(h_{wf} + h_{surf})}{\varphi} \tag{4}$$

where h_{wf} is the wetting front potential, which is also referred to as the effective capillary drive [*Morel-Seytoux et al*., 1996], capillary pull, or macroscopic capillary length [*White and Sully*, 1987]. The correction factor φ accounts for deviations from a sharp wetting front and/or viscous damping effects. For example, $\varphi = 1$ for a *Green and Ampt* [1911] solution, 1.1 for the *White and Sully* [1987] solution, and 1.1-1.7 for the *Morel-Seytoux and Khanji* [1974] solution.

[9] Because hydraulic conductivity is embedded in sorptivity, certain measurements of the latter can be used to infer the former. One such approach is to utilize field-based sorptivity measurements in conjunction with variations of the traditional sorptivity model [equation (4)] to quantify K_s [*White and Perroux*, 1987, 1989]. However, estimates of initial soil moisture and the soil's wetting front potential are needed for this approach. Solutions exist to quantify wetting front potential in dry soils (when $\Theta_0 = 0$) [*Rawls et al*., 1992; *Morel-Seytoux et al*., 1996], given that the parameters of a water retention function are known. For instance, *Morel-Seytoux et al*. [1996] approximated the wetting front potential of a dry soil as

$$h_{wf} = \left(\frac{1}{\alpha}\right)\left(\frac{0.046\,m + 2.07\,m^2 + 19.5\,m^3}{1 + 4.7\,m + 16\,m^2}\right) \tag{5}$$

where α and m are parameters of the *Van Genuchten* [1980] water retention curve, based on the *Mualem* [1976] water retention model, for $\alpha > 0$ and $0 < m < 1$.

[10] h_{wf} is recognized to change with the initial moisture state of the soil [*Green and Ampt*, 1911], and the aforementioned solutions for estimating wetting front potential do not include corrections for this variation. In a different approach, *Bouwer* [1964] and *Neuman* [1976] described h_{wf} at early infiltration times as a function of soil matric potential, h, by

$$h_{wf} = \frac{1}{2}\int_0^{h_0}\left(1 + \frac{\theta - \theta_0}{\theta_s - \theta_0}\right)K_r(h)dh \tag{6}$$

where $K_r(h)$ is the relative hydraulic conductivity function $K(h)/K_s$. While it is possible to put equation (6) in terms of Θ_0 by using a characteristic curve relationship [*Brooks and Corey*, 1964; *Van Genuchten*, 1980], the resulting equations are cumbersome.

[11] In this paper, we propose an alternative formulation of wetting front potential as a function of initial degree of saturation. This allows for a modification to the traditional (Green and Ampt) sorptivity model so that it better approximates sorptivity throughout the soil moisture range, including nearly saturated soils ($\Theta < 0.96$). This modified expression can then be used to interpret short-term constant head infiltration measurements, to quantify the magnitude and variability in time and space of a soil's saturated hydraulic conductivity, even in wet soils.

2. Theory

2.1. Sorptivity and Wetting Front Potential

[12] The *Parlange* [1975] expression for sorptivity in terms of soil diffusivity (D) and degree of saturation (Θ) is:

$$S^2 = (\theta_s - \theta_r)^2\int_{\Theta_0}^{\Theta_f}(\Theta_f + \Theta - 2\Theta_0)D(\Theta)d\Theta \tag{7}$$

where θ_f is the final volumetric soil water content.

[13] Soil diffusivity (D) is defined as

$$D = K\frac{dh}{d\theta} \tag{8}$$

and was approximated in terms of Θ by *Van Genuchten* [1980], using the *Mualem* [1976] water retention model, as:

$$D(\Theta) = \frac{(1-m)K_s}{\alpha m(\theta_s - \theta_r)}\Theta^{1/2-1/m}\left[\left(1 - \Theta^{1/m}\right)^{-m} + \left(1 - \Theta^{1/m}\right)^{m} - 2\right] \tag{9}$$

[14] It should be noted that using the *Mualem* [1976] model allows for estimation of the parameter m using the more commonly referenced parameter n through the relationship $m = 1 - 1/n$. By combining equations (7) and (9), sorptivity can be expressed for a soil with any initial water content as

$$S^2 = K_s(\theta_s - \theta_r)\frac{(1-m)}{\alpha m}\int_{\Theta_0}^{\Theta_f}(\Theta_f + \Theta - 2\Theta_0)\Theta^{1/2-1/m}\left[\left(1 - \Theta^{1/m}\right)^{-m} + \left(1 - \Theta^{1/m}\right)^{m} - 2\right]d\Theta \tag{10}$$

[15] For positive (ponded) pressure head [*Haverkamp et al*., 1990], (10) can be modified as

$$S^2 = K_s(\theta_s - \theta_r)\left\{2h_{surf}(1 - \Theta_0) + \frac{(1-m)}{\alpha m}\int_{\Theta_0}^{1}(1 + \Theta - 2\Theta_0)\Theta^{1/2-1/m}\left[\left(1 - \Theta^{1/m}\right)^{-m} + \left(1 - \Theta^{1/m}\right)^{m} - 2\right]d\Theta\right\} \tag{11}$$

[16] Equations (10) and (11) allow for accurate quantification of sorptivity throughout the soil moisture range. We

are now able to express the wetting front potential as a function of initial degree of saturation by equating equations (11) with (4) and then solving for h_{wf}:

$$h_{wf} = h_{surf}(\varphi - 1) + \left(\frac{(1-m)\varphi}{2\alpha m(1-\Theta_0)} \int_{\Theta_0}^{1} (1 + \Theta - 2\Theta_0) \Theta^{1/2-1/m} \left[\left(1 - \Theta^{1/m}\right)^{-m} + \left(1 - \Theta^{1/m}\right)^{m} - 2 \right] d\Theta \right) \quad (12)$$

[17] As an alternate approach, equations (10) and (11) can also be expressed in terms of the *Van Genuchten* [1980] equation based on the *Burdine* [1953] water retention model as

$$S^2 = K_s(\theta_s - \theta_r) \frac{(1-m)}{2\alpha m} \int_{\Theta_0}^{\Theta_f} (\Theta_f + \Theta - 2\Theta_0) \Theta^{\frac{3m-1}{2}} \left[\left(1 - \Theta^{1/m}\right)^{\frac{-m-1}{2}} - \left(1 - \Theta^{1/m}\right)^{\frac{m-1}{2}} \right] d\Theta \quad (13)$$

or for ponded conditions as

$$S^2 = K_s(\theta_s - \theta_r) \left\{ 2h_{surf}(1 - \Theta_0) + \frac{(1-m)}{2\alpha m} \int_{\Theta_0}^{1} (1 + \Theta - 2\Theta_0) \Theta^{\frac{3m-1}{2}} \left[\left(1 - \Theta^{1/m}\right)^{\frac{-m-1}{2}} - \left(1 - \Theta^{1/m}\right)^{\frac{m-1}{2}} \right] d\Theta \right\} \quad (14)$$

which is subject to the constraint $m = 1 - 2/n$.

[18] The van Genuchten-Burdine model has been shown to be more accurate for fine-textured soils (with low values of m) [*Fuentes et al*., 1992]. However, the van Genuchten-Maulem model enjoys widespread usage, serving as the basis for equation (5) and for numerical simulation models such as HYDRUS-1D [*Simunek et al*., 2005]. Thus, we will primarily make use of the sorptivity model based on the van Genuchten-Maulem parameters [equation (11)] throughout the remainder of our results and discussion. Analysis of the effect of water retention model choice on the calculation of wetting front potential is included as an Appendix A.

2.2. Nondimensional (Scaled) Sorptivity

[19] Numerous sorptivity solutions exist based on initially dry conditions, where $\Theta_0 = 0$ [e.g., *Brutsaert*, 1976]. This makes it advantageous to characterize soils in nondimensional terms, where a soil's actual sorptivity is scaled relative to its maximum (dry) sorptivity. Whereas the nondimensional forms of equations (11)–(14) require numerical evaluation, *Haverkamp et al*. [1998] provided an analytical function for relative sorptivity:

$$\frac{S^2}{S_{\max}{}^2} = \left(\frac{\theta_s - \theta_0}{\theta_s}\right)\left(\frac{K_s - K_0}{K_s}\right) \quad (15)$$

where K_0 is the initial (unsaturated) hydraulic conductivity. Using the common assumption that $\theta_r = 0$ [*Van Genuchten et al*., 1991; *Haverkamp et al*., 2005; *Canone et al*., 2008], equation (15) can be rewritten as

$$\frac{S^2}{S_{\max}{}^2} = (1 - \Theta_0)\left(1 - \frac{K_0}{K_s}\right) \quad (16)$$

[20] We now look to the *Brooks and Corey* [1964] expression for relative hydraulic conductivity

$$\frac{K_0}{K_s} = \Theta_0{}^{\eta} \quad \text{for } h < h_{cr} \quad (17)$$

where η is a pore size distribution index and h_{cr} is a parameter commonly associated with the air entry pressure.

[21] Combining equations (16) and (17) gives us:

$$\frac{S^2}{S_{\max}{}^2} = (1 - \Theta_0)(1 - \Theta_0{}^{\eta}) \quad \text{for } h < h_{cr} \quad (18)$$

3. Results and Discussion

[22] Equations (11) and (12) were integrated numerically to solve for sorptivity and wetting front potential, respectively, over the range $0 \leq \Theta_0 < 1$. Table 1 lists the seven soils analyzed, and their properties. The depth of ponding h_{surf} was assumed to be 0, which is a typical assumption for a single-ring infiltration test of short duration. The correction factor φ (used to account for deviations from a sharp wetting front and/or viscous damping effects) was set equal to 1, which corresponds to the Green-Ampt model. It should be noted the effect of φ on sorptivity and wetting front potential throughout the soil moisture range is beyond the scope of this work, but merits further exploration.

3.1 The Nature of Wetting Front Potential

[23] A soil's wetting front potential diminishes as its degree of saturation increases, with different rates of decrease between soil types (Figure 1). This results in a

Table 1. Parameters of the Seven Theoretical Soils Used for Comparison (From *Fuentes et al*. [1992])

Soil	θ_r	θ_s	α (cm^{-1})	m	n	η	K_s (cm h^{-1})
Grenoble Sand	0	0.312	0.0432	0.5096	2.039	4.553	15.37
Guelph Loam	0.2183	0.52	0.0115	0.5089	2.036	6.842	1.3167
Columbia Silt	0	0.401	0.0176	0.256	1.344	10.29	0.21
Yolo Light Clay	0	0.495	0.0324	0.208	1.263	12.64	0.0443
Beit Netofa Clay	0.2859	0.4460	0.00202	0.3725	1.594	18.33	0.0034
Touchet Silt Loam G.E.3	0.1903	0.4690	0.00505	0.8690	7.634	4.148	12.625
Hygiene Sandstone	0.1531	0.2500	0.00793	0.9035	10.363	3.678	4.5

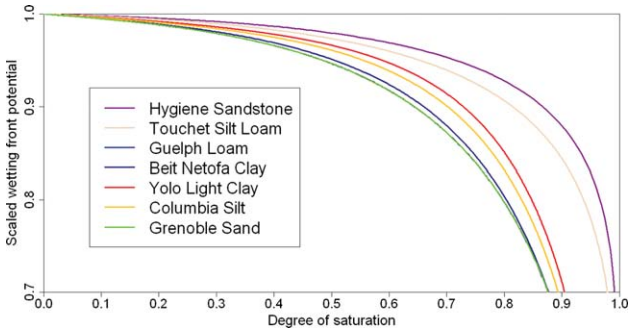

Figure 1. Scaled wetting front potential as a function of degree of saturation for the seven soils of Table 1. Values were calculated using equation (12).

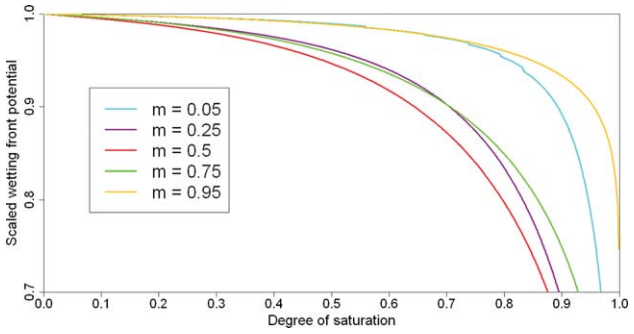

Figure 2. The effect of pore size distribution (m) on wetting front potential and sorptivity. Equations (4) and (13) give, respectively, the traditional and modified sorptivity models.

>50% difference in scaled wetting front potential as the soils neared saturation ($\Theta_0 = 0.96$). However, at the dry end of the curve ($0 < \Theta_0 < 0.5$), the scaled wetting front potential is nearly constant for the soil types, with a decrease from maximum values of <4% for all soil types. As such, the *Morel-Seytoux et al*. [1996] approximation (equation (5)) provides a suitable estimate of wetting front potential for this range (Table 2).

[24] The pore size distribution term (m) also strongly influences the wetting front potential (Figure 2). Soils with moderate pore size distributions ($0.2 < m < 0.8$) experienced the most pronounced drop in wetting front potential at high moisture content (Figure 2), with the largest effect occurring at $m = 0.5$ while soils with uniform pore size ($m = 1$) have a constant wetting front potential throughout the entire moisture range, and thus will behave as Green and Ampt soils. Since most soils have pore size distributions in the range $0.2 < m < 0.7$, the assumption of constant wetting front potential is poor, and equations such as (11) and (14) will provide better estimates of soil sorptivity in wet conditions.

[25] Traditionally, h_{wf} has been considered to be a capillary term, which would suggest that finer soils, having smaller pore sizes, will have greater wetting front potentials [*Swartzendruber et al*., 1954; *Selker et al*., 1999]. However, as can be seen in Figure 3 (where wetting front potential isolines are plotted as functions of van Genuchten parameters α and m), increasing the pore size distribution (decreasing m) reduces the wetting front potential. This is particularly notable for $m < 0.3$, and is the reason that Columbia Silt soil can have both α and h_{wf}, which are smaller than those of Grenoble Sand soil. Unlike the *Green and Ampt* [1911] and *Washburn* [1921] conceptual model of a bundle of tubes of varying radii, but with each individual tube having constant radii through its length, the Haines model [*Haines*, 1930] of soil filling and draining—where soil is idealized to be made up of a connected network of pore necks and pore bodies—may provide a partial physical explanation of this phenomenon. In the Haines model, capillarity will be controlled by the radii of the bodies of the largest connected pores, since the wetting front will not advance until those pore bodies have filled. Conversely, hydraulic conductivity will be governed by the necks of the smallest connected pores [*Hunt and Gee*, 2002]. Thus, for many soils, wetting front potential and sorptivity will both be smaller than predicted by traditional formulations such as the LaPlace and Poiseuille equations [*Washburn*, 1921; *Swartzendruber et al*., 1954; *Selker et al*., 1999].

3.2. Soil Moisture-Sorptivity Relationship

[26] Unlike wetting front potential, which demonstrated significant differences between soil textures, the scaled S^2 versus Θ_0 curves were similar throughout the range of initial soil moisture and across all soil types (Figure 4). Additionally, under relatively dry initial conditions (e.g. $\Theta_0 < 0.5$) the traditional sorptivity model in equation (4) accurately captures the proper sorptivity behavior. In soils with high initial water contents, however, the traditional model overestimates the value of sorptivity compared to the more accurate equation (11). This overestimation can exceed 50% for $\Theta_0 < 0.9$ over the range $0 < \Theta_0 < 0.9$, and approach 100% at $\Theta_0 = 0.95$, due to the decrease in wetting front potential observed at higher soil moistures.

[27] Therefore, to counter the overestimation of sorptivity in equation (4), we suggest multiplying the Θ_0 term of equation (4) by a correction factor γ:

Table 2. Wetting Front Potential (in cm) of Seven Theoretical Soils at Five Different Degrees of Initial Saturation[a]

Soil	$\Theta_0 = 0.0$	$\Theta_0 = 0.1$	$\Theta_0 = 0.3$	$\Theta_0 = 0.6$	$\Theta_0 = 0.9$	M-S
Grenoble Sand	9.22	9.18	9.03	8.46	6.10	9.64
Guelph Loam	34.6	34.4	33.9	31.8	23.0	36.1
Columbia Silt	7.98	7.95	7.85	7.49	5.51	8.29
Yolo Light Clay	3.08	3.07	3.04	2.92	2.20	3.18
Beit Netofa Clay	125.1	124.4	122.7	115.4	80.3	130.7
Touchet Silt Loam G.E.3	162.4	161.9	160.6	156.0	137.5	166.1
Hygiene Sandstone	109.1	108.9	108.2	105.5	95.5	111.0

[a]The column M-S uses the approximation of *Morel-Seytoux et al*. [1996] (equation (5)) for initially dry soils.

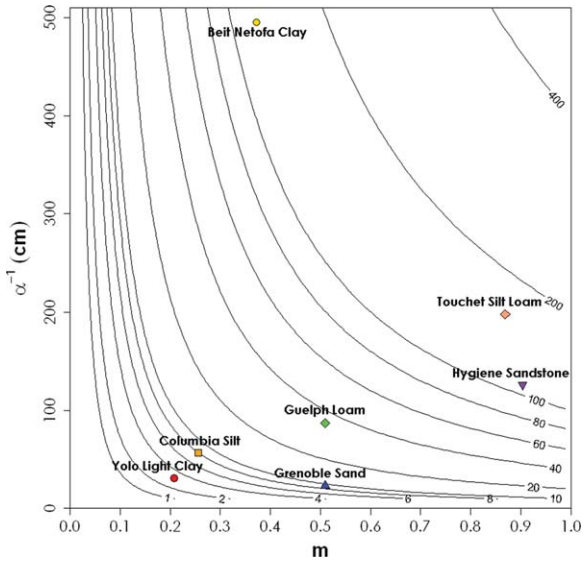

Figure 3. Wetting front potential isolines (in cm) for initially dry soils as a function of van Genuchten parameters α and m. The seven soils of Table 1 are plotted for reference.

$$S^2 = 2K_s(\theta_s - \theta_r)(1 - \gamma\Theta_0)(h_{wf} + h_{surf}) \tag{19}$$

or in nondimensional form:

$$\frac{S^2}{S_{\max}{}^2} = (1 - \gamma\Theta_0) \tag{20}$$

[28] When, for example, $\gamma = 1.025$, sorptivity estimates from equation (19) differ from those of equation (11) by $<20\%$ for all soils over the range $0 < \Theta_0 < 0.9$. At $\Theta_0 = 0.95$ the maximum deviation between equations (11) and (19) approaches 40%, although for most soil types, including the fine-textured silts and clays, the difference remains at $<20\%$ (Figure 4 inset).

3.3. Soil Matric Potential Relationships

[29] S^2 was also plotted as a function of the soil matric potential, h, using the relationship proposed by *Van Genuchten* [1980]:

$$\Theta = \left(\frac{1}{1 + (\alpha h)^n}\right)^m \tag{21}$$

[30] The S^2 versus h curves vary in scale across soil types (Figure 5). Further, as seen in Appendix A, the choice of water retention model can affect the magnitude of the scaled soil matric potential. Thus, for our application it is preferable to describe sorptivity using Θ rather than h.

3.4. Nondimensional (Scaled) Sorptivity

[31] Nondimensional (scaled) sorptivity was compared for four of the theoretical soils (Yolo Light Clay, Beit Netofa Clay, Guelph Loam and Hygiene Sandstone) using equations (11), (14), (18), and (20). Each model predicted a different behavior in wet soil conditions (Figure 6). The van Genuchten-Maulem [equation (11)] and van Genuchten-Burdine [equation (14)] models had similar curve shapes,

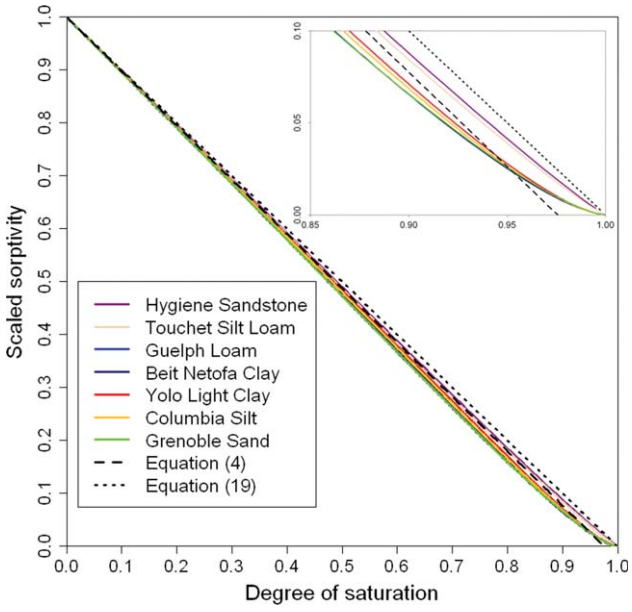

Figure 4. Scaled sorptivity as a function of degree of saturation for the seven theoretical soils. The inset highlights the wet end of the curve, near saturation. Equation (4)—i.e., the traditional Green-Ampt sorptivity model—and equation (11), i.e., the modified Green-Ampt sorptivity model, are also shown.

with an offset that increased as the pore size distribution parameter m became smaller. In the case of the Hygiene Sandstone soil, where m is near 1, the two curves were indistinguishable.

[32] The modified Haverkamp model [equation (18)], conversely, demonstrated the greatest offset in soils with near-uniform pore size distributions (high values of m), such as the Hygiene Sandstone. This is likely due to the air entry pressure (h_{cr}) being an important term in these coarse

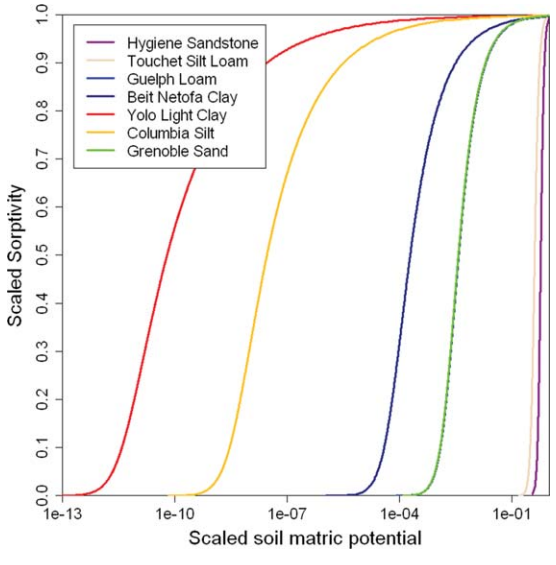

Figure 5. Scaled sorptivity as a function of scaled soil potential for the seven theoretical soils. Note that the Guelph Loam and Grenoble Sand soils have nearly identical curves.

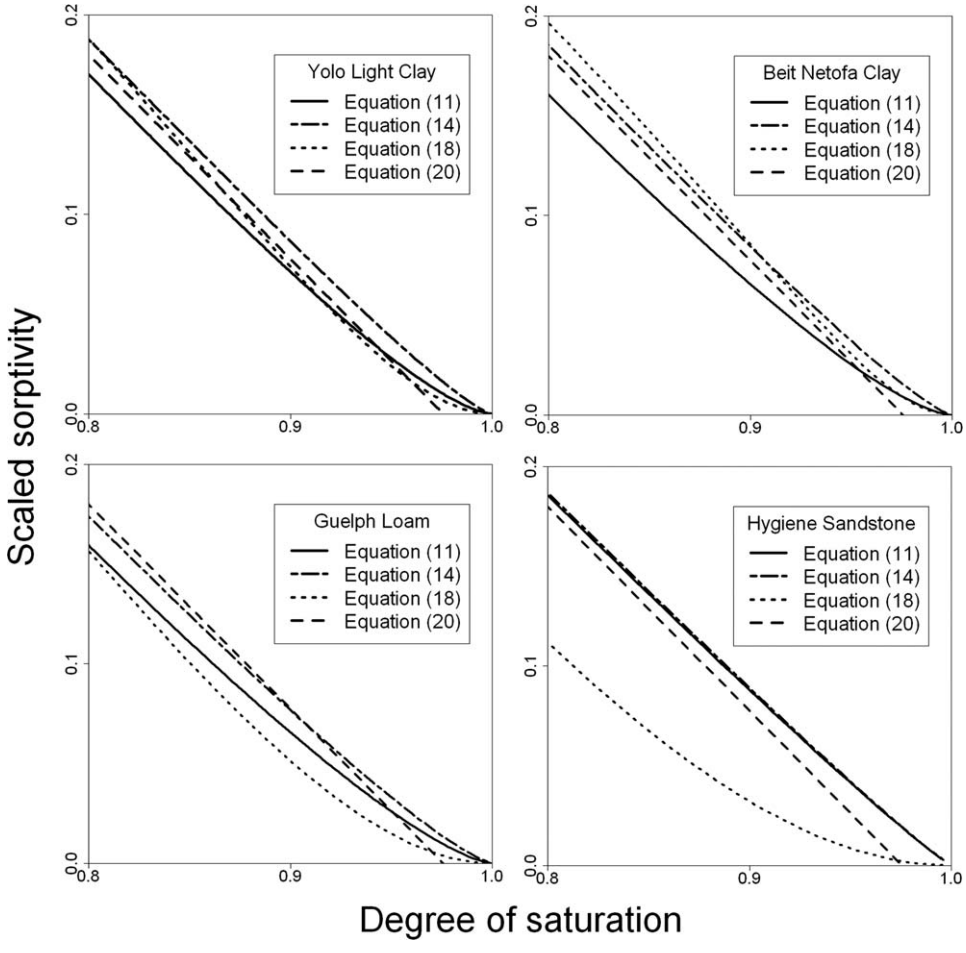

Figure 6. Comparison of scaled sorptivity ($S2/S2max$) predicted for four theoretical soils in wet conditions (degree of saturation $\Theta > 0.8$). The four lines shown correspond to: equation (11), the van Genuchten-Maulem model; equation (14), the van Genuchten-Burdine model; equation (18), the modified Haverkamp model; and equation (20), the modified Green-Ampt model.

soils, and implies that the Brooks and Corey relative hydraulic conductivity function [equation (17)] may be a poor choice to predict the sorptivity of coarse soils as they near saturation. However, as the pore size distribution became wider (m becoming smaller), the modified Haverkamp model predicted scaled sorptivity values which fell between the two van Genuchten models. Thus, equation (18) can be considered to be a suitable sorptivity approximation for fine-textured soils ($m > 0.4$).

[33] Although a simple linear function that is independent of soil type, equation (20) closely approximated the scaled sorptivity predicted by the van Genuchten models over the range of soils tested, including the coarse-textured soils. Equation (20) therefore represents a suitable approximation for the scaled sorptivity of most real soils, with the additional advantage of not requiring an estimate of the pore-size distribution index.

4. Application–Determining Saturated Hydraulic Conductivity From Sorptivity

[34] Sorptivity measurements can be used to quantify hydraulic conductivity by, for instance, combining equations (5) and (19)

$$K_s = \left(\frac{S^2\alpha\varphi}{(\theta_s - \theta_r)(1-\gamma\Theta_0)}\right)\left(\frac{1+4.7m+16m^2}{0.092m+4.14m^2+39m^3}\right) \quad (22)$$

where m is subject to the constraint $m = 1 - 1/n$ (i.e., the van Genuchten-Maulem model).

[35] Equation (22) allows for early-time infiltration data, such as can be obtained with single-ring tests, to be used to estimate K_s. This was verified through numerical simulations of one-dimensional horizontal infiltration for five of the soils listed in Table 1, at five different initial water contents ($\Theta_0 = 0$, 0.1, 0.3, 0.6, and 0.9) using the HYDRUS-1D model. The model domain was 5 m in length, with a node spacing of 0.01 m. The origin boundary condition was set as $\theta = \theta_s$ and the far boundary was set as no flux. For early times, when the water content of the far boundary varied by <1%, sorptivity was calculated from the water flux, i, through the origin by using $S = 2i\ (t^{0.5})$. The scaling parameter φ was assumed to be 1 and γ was assumed to be 1.025.

[36] Equation (22) predicted the K_s values for all five soils under all five initial degrees of saturation (Table 3) with errors under 20%. The error was minimal for the dry soils, ranging from 0.6 to 4.6% for $\Theta_0 = 0.1$ and 0.3. For

Table 3. Saturated Hydraulic Conductivities (K_s) Used as Input Parameters, Versus Those Calculated by Equation (13), for Four Different Initial Degrees of Saturation (Units Are in cm h^{-1})[a]

		K_s Calculated–Equation (13)			
Material	K_s Actual	$\Theta_0 = 0.1$	$\Theta_0 = 0.3$	$\Theta_0 = 0.6$	$\Theta_0 = 0.9$
Grenoble Sand	15.4	15.0	15.1	14.6	12.8
Guelph Loam	1.32	1.29	1.31	1.27	1.21
Columbia Silt	0.210	0.203	0.201	0.200	0.180
Yolo Light Clay	0.0443	0.0439	0.0423	0.0414	0.0388
Hygiene Sandstone	4.5	4.4	4.4	4.5	7.5

[a]Absolute error ranged from ~2% for dry soils to 17% for infiltration into wet sand. The solution poorly estimated the hydraulic conductivity for Hygiene Sandstone at $\Theta_0 = 0.9$, because of divergence in the sorptivity as calculated by HYDRUS-1D and by equation (9).

the wettest soils ($\Theta_0 = 0.9$), the error increased (ranging from 8.1 to 17%), but nevertheless would allow rapid determination of saturated hydraulic conductivity which typically spans an order of magnitude for multiple samples of the same soil [*Nielsen et al*., 1973]. Using a soil specific value of φ could also be used to account for deviations in the wetting front shape between soils and improve estimates of K_s. It should be noted that for the Hygiene Sandstone soil at $\Theta_0 = 0.9$, equation (22) overestimated K_s by nearly a factor of two, due to the divergence of the analytical sorptivity solution [equation (11)] and the HYDRUS-1D numerical solution. This can also be seen in Figure 7, which shows sorptivity values predicted by both equation (11) and HYDRUS-1D.

[37] Although equation (22) requires sorptivity and initial degree of saturation to be measured, as well as knowledge of soil parameters θ_s, θ_r, α, and m, this represents a reduction of data needed compared to other methods. For example, the Beerkan Method [*Braud et al*., 2005] requires estimates of the initial and final volumetric water contents, bulk density, and the final depth of wetting for each infiltration test.

[38] Further, K_s has been shown to exhibit greater spatial variability than α, m, θ_r, or θ_s, with θ_s and m possessing the least spatial variability [*Mallants et al*., 1996]. This signifies that for any single location, the denominator of equation (22) can be constrained using few soil samples relative to the number of infiltration tests. This in turn makes it possible to use simple infiltration tests (such as the single ring infiltrometer) to quantify the spatial distribution of K_s in a single soil type.

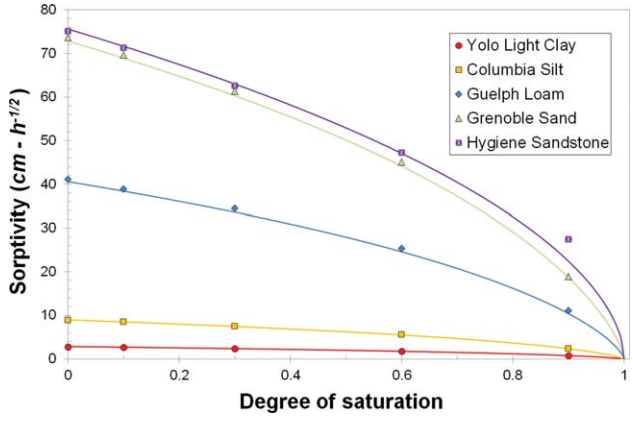

Figure 7. Sorptivity versus initial degree of saturation for five of the theoretical soils. The lines are calculated using equation (9), while the points are based on HYDRUS-1D simulations.

5. Application–Sorptivity Isolines

[39] A practical application of equations (11), (13), (18), and/or (20) is to generate theoretical sorptivity isolines against which to compare sorptivity estimates taken at various initial soil moisture contents. Deviations from theory in soil properties under different moisture contents could point to hysteresis in properties of a rigid soil, while in swelling soils this could be used to examine the variability of the effective hydraulic conductivity.

[40] To demonstrate the application of these methods, a set of single-ring infiltration experiments were conducted monthly from September 2011 to March 2013 near Corvallis, Oregon. Measurements were taken at 12 points within a 2 × 3 m open field area, with native pasture cover. The soil was identified as a Waldo silty clay loam (*fine, smectitic, mesic Fluvaquentic Vertic Endoaquoll*), with moderate to high shrink-swell potential [*Knezevich*, 1975]; 0.09 m diameter rings were installed to 0.01 m depth. The small diameter of the rings allowed them to be placed away from large surface-connected cracks and thereby infiltrate through the soil matrix. Up to 1 L of water (with a minimum of 0.4 L) was added to each ring in 0.1 L increments, and the time between the 0.1 L pours were recorded.

[41] Sorptivity was estimated using the early-time approximation for the first 0.4 L, where $S = I(t^{-0.5})$ [*White et al*., 1992], and is presented as a mean and standard deviation of all 12 points on a single date. Due to the short duration of the infiltration tests (lasting from >1 to ~20 min in dry conditions and >1−4 h in wet conditions), it was assumed that material swelling was not significant and that the early time approximation was valid.

[42] Mean initial degree of saturation was determined from six soil cores taken within the grid on each sampling date, and was calculated for each sample by dividing the moisture ratio, ϑ, by the void ratio, e.

$$\Theta_0 = \frac{\vartheta}{e} = \left(\frac{V_w/V_s}{V_v/V_s}\right) = \frac{V_w}{V_v} = \left(\frac{(m_0\text{-}m_{dry})/\rho_w}{V_0\text{-}(m_{dry}/\rho_s)}\right) \qquad (23)$$

where V_w is the volume of water; V_s the volume of solids; V_v the volume of voids; m_0 the mass; m_{dry} the mass after 24 h drying at 105°C; ρ_w the density of water; V_0 the original volume; and ρ_s the density of the solids (assumed to be 2.67 g cm^{-3}).

[43] The initial measurements were taken in relatively dry soils. It was observed that as the soils wetted the apparent saturated hydraulic conductivity decreased, to ~50% of the original (Figure 8). As the soil redried hysteresis was observed, with the effective saturated hydraulic conductivity 2.5 greater than the original value, even at similar initial degrees of saturation. This was likely due to hysteretic soil shrinkage, including opening of new cracks within the single-ring sampling areas. While more information about

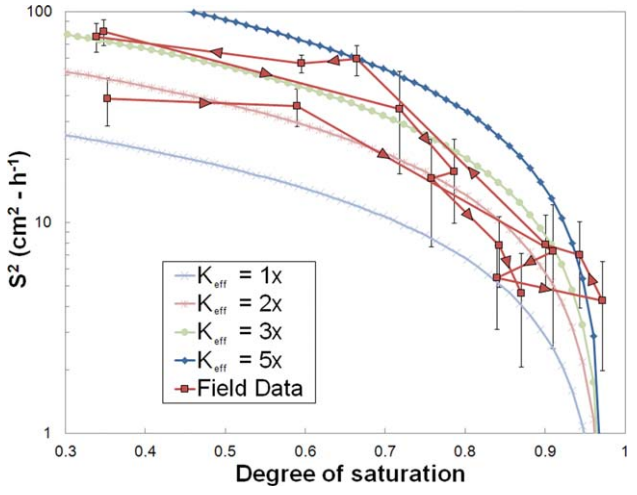

Figure 8. Sorptivity isolines based on the relationship between sorptivity and initial degree of saturation (using equation (10) and assuming $h_{surf} = 0$). The isolines represent the expected sorptivity of a soil with a constant saturated hydraulic conductivity. The field data come from a soil with vertic (shrink-swell) properties, which has varying effective hydraulic conductivity (K_{eff}) as macropores open and close. Sorptivity was estimated using the early time approximation of *White et al*. [1992]. The arrows indicate chronological progression of estimates sorptivity taken at different times of the year (resulting in different initial soil moisture contents).

the soil parameters would be needed to use equation (22), the isolines generated by equations (11), (14), (18), or (20) are useful for identifying qualitative shifts in soil properties, and in this example demonstrated that the effective saturated hydraulic conductivity of a cracking soil was neither constant nor unique as the soils wetted and dried.

6. Summary and Conclusions

[44] Sorptivity can be calculated by use of a diffusivity function, such as the *Parlange* [1975] formulation, or by use of a combination of conductivity and capillarity terms, such as the *Green and Ampt* [1911] sorptivity model. Equating these two formulae allowed exploration of the capillarity (as wetting front potential) term in Green and Ampt-type models as a function of initial soil moisture and the water retention function [*Van Genuchten*, 1980]. It was determined that a soil's pore size distribution greatly influenced both the magnitude of the wetting front potential term, as well as the rate at which the wetting front potential decreased as soil moisture increased. For instance, soils with wide pore size distributions had diminished wetting front potentials relative to soils with more uniform pore sizes, whereas soils with moderate pore size distributions experienced the most rapid decrease in wetting front potential at higher water contents. However, the variability in wetting front potential characteristics had little influence on sorptivity, as it was determined that the relationship between sorptivity and initial degree of saturation could be predicted nearly independent of soil type. This observation allowed for calculation of sorptivity even in wet soils, and permitted a minor linear correction to the traditional (i.e., Green-Ampt) model of sorptivity to improve its accuracy throughout the entire range of soil moisture.

[45] The modified Green-Ampt model was compared with the *Parlange* [1975] and *Haverkamp et al*. [1998] expressions, where the latter was modified through inclusion of the *Brooks and Corey* [1964] relative hydraulic conductivity expression. Sorptivity predicted by the modified Green-Ampt model was accurate for the soil moisture range $0 \leq \Theta < 0.96$, while the modified Haverkamp expression covered the entire moisture range, though with a divergent behavior in coarse soils such as sand (likely due to limitations of the Brooks and Corey expression). Since the sorptivity of wet soils can be difficult to accurately measure, these expressions should prove useful for modeling infiltration and flow in such conditions.

[46] These results also allow determination of saturated hydraulic conductivity from simple single ring infiltration tests, requiring only an estimate of the initial degree of saturation and the soil's water retention curve parameters. This represents a simplification of standard methods for interpreting such infiltration tests, and the solution is valid even for wet soils, provided a satisfactory measurement of the soil sorptivity can be made in such conditions. The formulae proposed in this study are particularly useful for fine-textured soils due to their tendency to retain moisture (and therefore have non-zero initial water contents) and to be restrictive to flow (making it difficult to attain the steady-state conditions necessary to utilize many infiltration models).

[47] Altogether, the findings presented here enable us to monitor changes in soil properties such as can occur during wetting and drying, to examine rainfall-runoff relationships in wet soils, and to better quantify and predict water movement in many soil types.

Appendix A: Water Retention Model Influence on Predicted Wetting Front Potential

[48] *Van Genuchten* [1980] described soil diffusivity, D, using two different water retention models. The first, based on the work of *Mualem* [1976], allows for diffusivity to be written as:

$$D(\Theta) = \frac{(1-m)K_s}{\alpha m(\theta_s - \theta_r)}\Theta^{1/2-1/m}\left[\left(1-\Theta^{1/m}\right)^{-m} + \left(1-\Theta^{1/m}\right)^{m} - 2\right] \tag{24}$$

which, when combined with the *Parlange* [1975] and *Green and Ampt* [1911] sorptivity models, allows for wetting front potential to be expressed as:

$$h_{wf} = h_{surf}(\varphi - 1) + \left(\frac{(1-m)\varphi}{2\alpha m(1-\Theta_0)}\int_{\Theta_0}^{1}(1+\Theta-2\Theta_0)\Theta^{1/2-1/m}\left[\left(1-\Theta^{1/m}\right)^{-m} + \left(1-\Theta^{1/m}\right)^{m} - 2\right]d\Theta\right) \tag{25}$$

where m can be related to the more commonly referenced parameter n by $m = 1 - 1/n$.

Table A1. Parameters of the Seven Theoretical Soils (From *Fuentes et al*. [1992]), Along With Calculated Maximum Wetting Front Potential, Based on the *Mualem* [1976] and *Burdine* [1953] Models

	Maulem [1976]				Burdine [1953]				
Soil	α^{-1} (cm)	m	n	h_{wf} (cm)	α^{-1} (cm)	m	n	h_{wf} (cm)	h_{wf} Difference[a]
Grenoble Sand	23.16	0.5096	2.039	9.22	16.39	0.2838	2.792	8.00	14%
Guelph Loam	86.96	0.5089	2.036	34.6	62.50	0.2888	2.812	31.1	11%
Columbia Silt	56.95	0.256	1.344	7.98	36.06	0.1248	2.285	9.44	17%
Yolo Light Clay	30.82	0.208	1.263	3.08	19.31	0.0995	2.221	4.16	30%
Beit Netofa Clay	495.81	0.3725	1.594	125.1	282.13	0.1198	2.272	71.3	55%
Touchet Silt Loam G.E.3	198.04	0.8690	7.634	162.4	192.01	0.7297	7.399	157.0	3%
Hygiene Sandstone	126.13	0.9035	10.363	109.1	124.41	0.8123	10.655	107.9	1%

[a] h_{wf} difference is calculated as $2 \times 100 \times (Maulem - Burdine)/(Maulem + Burdine)$.

[49] The second water retention model, based on the work of *Burdine* [1953], enables diffusivity to be expressed as:

$$D(\Theta) = \frac{(1-m)K_s}{2\alpha m(\theta_s - \theta_r)}\Theta^{\frac{3m-1}{2}}\left[\left(1-\Theta^{1/m}\right)^{\frac{-m-1}{2}} - \left(1-\Theta^{1/m}\right)^{\frac{m-1}{2}}\right] \tag{26}$$

which in turn provides the following expression for wetting front potential:

$$h_{wf} = h_{surf}(\varphi - 1) + \left(\frac{(1-m)\varphi}{4\alpha m(1-\Theta_0)}\int_{\Theta_0}^{1}(1+\Theta-2\Theta_0)\Theta^{\frac{3m-1}{2}}\left[\left(1-\Theta^{1/m}\right)^{\frac{-m-1}{2}} - \left(1-\Theta^{1/m}\right)^{\frac{m-1}{2}}\right]d\Theta\right) \tag{27}$$

where m can be related to the more commonly referenced parameter n by $m = 1 - 2/n$.

[50] Again, we will focus on seven distinct soil types, whose properties were characterized by *Fuentes et al*. [1992] (Table 3). Looking at initially dry soil conditions ($\Theta_0 = 0$), subtle differences are seen in the wetting front potential contour lines predicted by equations (12) and (27) (Figure A1). Much of the deviation in contour line location can be explained by the different definitions of the parameter m used for either model. However, at low values of m (representing soils with wide pore size distributions), the wetting front potentials predicted by the two models diverge. The Beit Netofa clay, for example, has a difference of >50% between wetting front potentials predicted by the Maulem and Burdine models.

[51] The two water retention models also predict different behaviors for the seven soils over the entire range of initial soil moisture $0 \le \Theta_0 < 1$ (Figure A2). In wet conditions ($\Theta_0 > 0.6$), the Maulem model shows pronounced differences between the various soil types in both the amount and rate of decreased wetting front potential. This translates to a

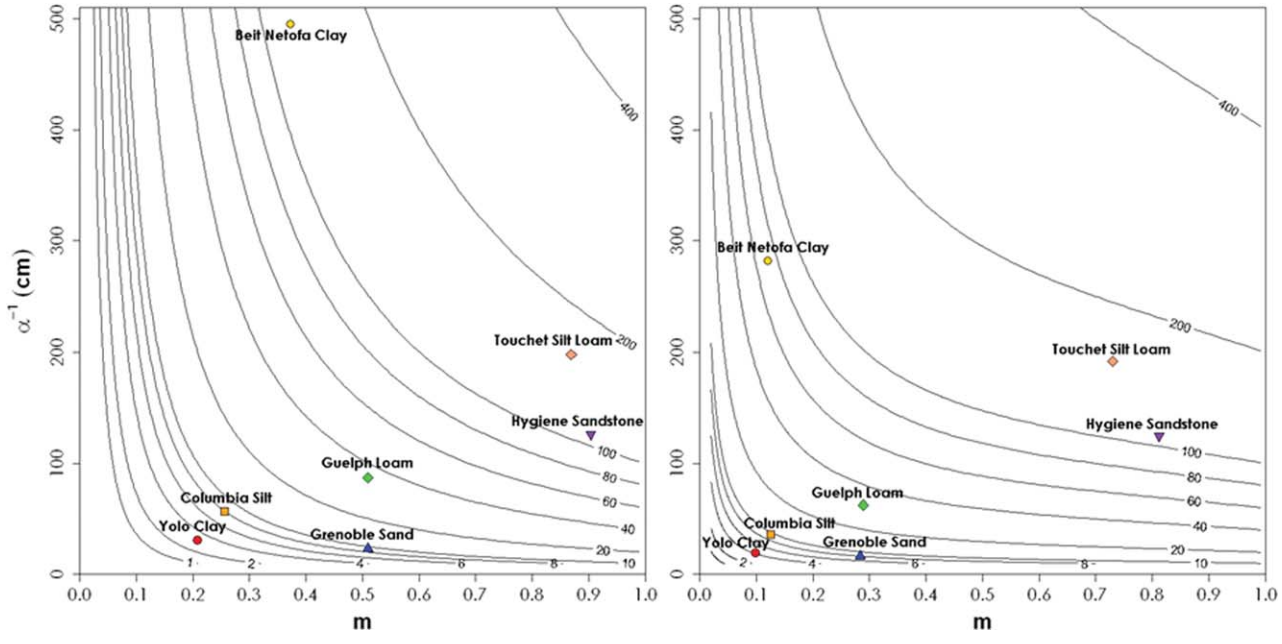

Figure A1. Wetting front potential (drawn as contour lines, with units of cm) as a function of van Genuchten parameters m and $\alpha - 1$ using: (at left) the *Maulem* [1976] water retention model (equation (12)); and (at right) the *Burdine* [1953] water retention model (equation (27)). The seven soils of Table 3 are plotted for reference.

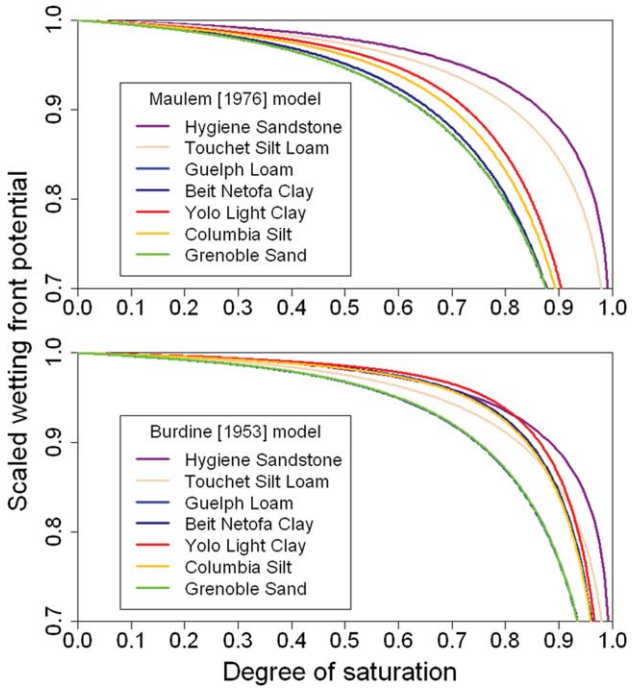

Figure A2. Scaled wetting front potential as a function of degree of saturation for the seven soils of Table A1.

maximum difference between soil types of 30% at $\Theta_0 = 0.9$ and 45% at $\Theta_0 = 0.95$. The Burdine model predicts a more uniform response between soil types, with a maximum deviation approximately one-half that of the Maulem model (14% at $\Theta_0 = 0.9$ and 24% at $\Theta_0 = 0.95$). Thus, the Burdine water retention model may be more amenable to creation and usage of a single-parameter function, which predicts the scaled wetting front potential independent of soil type.

[52] In summary, the predicted magnitude and moisture-dependent behavior of wetting front potential differ between the Maulem and Burdine water retention models. For most soils and practical purposes, the difference will be negligible and either model should suffice. For fine-textured soils with wide pore size distributions (low values of *m*), however, the models begin to diverge, which can have significant consequences on predicted wetting front potential. The van Genuchten-Burdine retention model has previously been demonstrated to be more accurate in soils with low *m* values [*Fuentes et al*., 1992], while the van Genuchten-Maulem retention model has previously been more widely used, resulting in a number of relevant and practical applications. We will leave it to the reader, then, to decide which model to employ based on his/her specific intent and desired outcome.

[53] **Acknowledgments.** This work has been supported under National Science Foundation award 0943682. The authors would like to thank the anonymous reviewers who provided helpful feedback and improved the quality and scope of this manuscript.

References

Bouwer, H. (1964), Unsaturated flow in ground-water hydraulics, *J. Hydr. Div., Proc. Am. Soc. Civil Eng.*, *90*(HY5), 121–144.

Braud, I., D. De Condappa, J. M. Soria, R. Haverkamp, R. Angulo-Jaramillo, S. Galle, and M. Vauclin (2005), Use of scaled forms of the infiltration equation for the estimation of unsaturated soil hydraulic properties (the Beerkan method), *Eur. J. Soil Sci.*, *56*(3), 361–374.

Brooks, R. H. and A. T. Corey (1964), Hydraulic properties of porous media, Hydrology Papers, Colorado State University.

Burdine, N. (1953), Relative permeability calculations from pore size distribution data, *Trans. Am. Inst. Min. Metall. Eng.*, *5*(3), 71–78.

Brutsaert, W. (1976), The concise formulation of diffusive sorption of water in a dry soil, *Water Resour. Res.*, *12*(6), 1118–1124.

Brutsaert, W. (1977), Vertical infiltration in dry soil, *Water Resour. Res.*, *13*(2), 363–368.

Canone, D., S. Ferraris, G. Sander, and R. Haverkamp (2008), Interpretation of water retention field measurements in relation to hysteresis phenomena, *Water Resour. Res.*, *44*, W00D12, doi:10.1029/2008WR007068.

Fuentes, C., R. Haverkamp, and J. Y. Parlange (1992), Parameter constraints on closed-form soilwater relationships, *J. Hydrol.*, *134*(1), 117–142.

Green, W. H. and G. Ampt (1911), Studies on soil physics, *J. Agric. Sci.*, *4*(1), 1–24.

Haines, W. B. (1930), Studies in the physical properties of soil. V. The hysteresis effect in capillary properties, and the modes of moisture distribution associated therewith, *J. Agric. Sci.*, *20*(01), 97–116.

Haverkamp, R., J.-Y. Parlange, J. Starr, G. Schmitz, and C. Fuentes (1990), Infiltration under ponded conditions: 3. A predictive equation based on physical parameters, *Soil Sci.*, *149*(5), 292–300.

Haverkamp, R., P. Ross, K. Smettem, and J. Parlange (1994), Three-dimensional analysis of infiltration from the disc infiltrometer: 2. Physically based infiltration equation, *Water Resour. Res.*, *30*(11), 2931–2935.

Haverkamp, R., F. Bouraoui, C. Zammit, and R. Angulo-Jaramillo (1998), Soil properties and moisture movement in the unsaturated zone, in *Handbook of Groundwater Engineering*, edited by J. Delleur, CRC Press, Boca Raton, Florida.

Haverkamp, R., F. J. Leij, C. Fuentes, A. Sciortino, and P. Ross (2005), Soil water retention I: Introduction of a shape index, *Soil Sci. Soc. Am. J.*, *69*(6), 1881–1890.

Hunt, A. G. and G. W. Gee (2002), Application of critical path analysis to fractal porous media: Comparison with examples from the Hanford site, *Adv. Water Resour.*, *25*(2), 129–146.

Knezevich, C.A. (1975), Soil Survey of Benton County Area, Oregon, US Soil Conservation Service.

Mallants, D., B. P. Mohanty, D. Jacques, and J. Feyen (1996), Spatial variability of hydraulic properties in a multi-layered soil profile, *Soil Sci.*, *161*(3), 167.

Morel-Seytoux, H. J. and J. Khanji (1974), Derivation of an equation of infiltration, *Water Resour. Res.*, *10*(4), 795–800.

Morel-Seytoux, H. J., P. D. Meyer, M. Nachabe, J. Touma, M. T. van Genuchten, and R. J. Lenhard (1996), Parameter equivalence for the Brooks-Corey and van Genuchten soil characteristics: Preserving the effective capillary drive, *Water Resour. Res.*, *32*(5), 1251–1258.

Mualem, Y. (1976), A new model for predicting the hydraulic conductivity of unsaturated porous media, *Water Resour. Res.*, *12*(3), 513–522.

Neuman, S. P. (1976), Wetting front pressure head in the infiltration model of Green and Ampt, *Water Resour. Res.*, *12*(3), 564–566.

Nielsen, D. R., J. W. Biggar, and K. T. Erh (1973), Spatial variability of field-measured soil-water properties, *Hilgardia*, *42*, 215–259.

Parlange, J. Y. (1975), On solving the flow equation in unsaturated soils by optimization: Horizontal infiltration, *Soil Sci. Soc. Am. J.*, *39*(3), 415–418.

Philip, J. R. (1957a), The theory of infiltration: 2. The profile of infinity, *Soil Sci.*, *83*(6), 435.

Philip, J. R. (1957b), The theory of infiltration: 4. Sorptivity and algebraic infiltration equations, *Soil Sci.*, *84*(3), 257.

Philip, J. R. (1990), Inverse solution for one-dimensional infiltration, and the ratio a/K1, *Water Resour. Res.*, *26*(9), 2023–2027.

Rawls, W. J., L. R. Ahuja, D. L. Brakensiek, A. Shirmohammadi, and D. Maidment (1992), *Infiltration and Soil Water Movement*, McGraw-Hill Inc., N. Y.

Selker, J. S., C. K. Keller, and J. T. McCord (1999), *Vadose Zone Processes*, 339 pp., Lewis Publishers, Boca Raton, Fla.

Simunek, J., M. T. Van Genuchten, and M. Sejna (2005), The HYDRUS-1D software package for simulating the one-dimensional movement of water, heat, and multiple solutes in variably-saturated media, *Res. Rep. 240*, Univ. of Calif., Riverside, Calif.

Smettem, K. R., P. Ross, R. Haverkamp, and J. Y. Parlange (1995), Three-dimensional analysis of infiltration from the disk infiltrometer: 3. Parameter estimation using a double-disk tension infiltrometer, *Water Resour. Res.*, *31*(10), 2491–2495.

Smiles, D. and J. Knight (1976), A note on the use of the Philip infiltration equation, *Soil Res.*, *14*(1), 103–108.

Swartzendruber, D., M. F. De Boodt, and D. Kirkham (1954), Capillary intake rate of water and soil structure, *Soil Sci. Soc. Am. J.*, *18*(1), 1–7.

Touma, J., M. Voltz, and J. Albergel (2007), Determining soil saturated hydraulic conductivity and sorptivity from single ring infiltration tests, *Eur. J. Soil Sci.*, *58*(1), 229–238.

Van Genuchten, M. T. (1980), A closed-form equation for predicting the hydraulic conductivity of unsaturated soils, *Soil Sci. Soc. Am. J.*, *44*(5), 892–898.

Van Genuchten, M. T., F. Leij, and S. Yates (1991), The RETC code for quantifying the hydraulic functions of unsaturated soils. *Tech. Report* EPA/600/2–91/065, US Environment Protection Agency.

Vandervaere, J. P., M. Vauclin, and D. E. Elrick (2000), Transient flow from tension infiltrometers: I. The Two-Parameter Equation, *Soil Sci. Soc. Am. J.*, *64*(4), 1263–1272.

Washburn, E. W. (1921), The dynamics of capillary flow, *Phys. Rev.*, *17*(3), 273–283.

White, I. and K. Perroux (1987), Use of sorptivity to determine field soil hydraulic properties, *Soil Sci. Soc. Am. J.*, *51*(5), 1093–1101.

White, I. and K. Perroux (1989), Estimation of unsaturated hydraulic conductivity from field sorptivity measurements, *Soil Sci. Soc. Am. J.*, *53*, 324–329.

White, I. and M. Sully (1987), Macroscopic and microscopic capillary length and time scales from field infiltration, *Water Resour. Res.*, *23*(8), 1514–1522.

White, I., M. Sully, and K. Perroux (1992), Measurement of surface-soil hydraulic properties: Disk permeameters, tension infiltrometers, and other techniques, in *Advances in Measurement of Soil Physical Properties: Bringing Theory into Practice*, pp. 69–103, Soil Science Society of America, Madison, Wis.

Wooding, R. (1968), Steady infiltration from a shallow circular pond, *Water Resour. Res.*, *4*, 1259–1273.